Alamethicin Topology in Phospholipid Membranes by Oriented Solid-state NMR and EPR Spectroscopies: a Comparison

Evgeniy S. Salnikov,[†,‡] Marta De Zotti,[§] Fernando Formaggio,[§] Xing Li,[||] Claudio Toniolo,[§] Joe D. J. O'Neil,[||] Jan Raap,[⊥] Sergei A. Dzuba,*[,†] and Burkhard Bechinger*[,‡]

Institute of Chemical Kinetics and Combustion, Russian Academy of Sciences, 630090 Novosibirsk, Russian Federation, University of Strasbourg/CNRS, UMR7177, Institut de Chimie, 67070 Strasbourg, France, Institute of Biomolecular Chemistry, CNR, Padova Unit, Department of Chemistry, University of Padova, 35131 Padova, Italy, Department of Chemistry, University of Manitoba, Winnipeg, Canada R3T 2N2, and Leiden Institute of Chemistry, Gorlaeus Laboratories, Leiden University, 2300 RA Leiden, The Netherlands

Received: November 19, 2008; Revised Manuscript Received: January 9, 2009

Alamethicin, a hydrophobic peptide that is considered a paradigm for membrane channel formation, was uniformly labeled with ^{15}N, reconstituted into oriented phosphatidylcholine bilayers at concentrations of 1 or 5 mol %, and investigated by solid-state NMR spectroscopy as a function of temperature. Whereas the peptide adopts a transmembrane alignment in POPC bilayers at all temperatures investigated, it switches from a transmembrane to an in-plane orientation in DPPC membranes when passing the phase transition temperature. This behavior can be explained by an increase in membrane hydrophobic thickness and the resulting hydrophobic mismatch condition. Having established the membrane topology of alamethicin at temperatures above and below the phase transition, ESEEM EPR was used to investigate the water accessibility of alamethicin synthetic analogues carrying the electron spin label TOAC residue at one of positions 1, 8, or 16. Whereas in the transmembrane alignment the labels at positions 8 and 16 are screened from the water phase, this is only the case for the latter position when adopting an orientation parallel to the surface. By comparing the EPR and solid-state NMR data of membrane-associated alamethicin it becomes obvious that the TOAC spin labels and the cryo-temperatures required for EPR spectroscopy have less of an effect on the alamethicin−POPC interactions when compared to DPPC. Finally, at P/L ratios of 1/100, spectral line broadening due to spin−spin interactions and thereby peptide oligomerization within the membrane were detected for transmembrane alamethicin.

Introduction

Alamethicin is a 19-mer peptide, acetylated at the N-terminus and extended with the 1,2-amino alcohol Phl at the C-terminus, produced by the fungus *Trichoderma viride* that generates a voltage-dependent conductance in bilayers [reviewed in refs 1−4]. It is of interest both as a model for voltage-gated channels and for the behavior of membrane-associated helices. Alamethicin is composed mostly of hydrophobic residues and adopts a predominantly helical structure in membrane-like environments.[5−7] The single-channel properties and the concentration dependence of the conduction are consistent with various degrees of helix oligomerization in the membrane.[8,9]

Alamethicin strongly associates with model membranes and exhibits a cooperative binding to fluid phase phosphatidylcholines as determined by both CD and EPR techniques.[10,11] The open alamethicin pore remains a paradigm for transmembrane helical bundles or barrel staves, which is a model consistent with the behavior of covalently linked alamethicin dimers.[12] However, CW EPR measurements at room temperature of C-terminally labeled alamethicin analogues failed to detect the postulated oligomeric state.[11,13,14]

When membrane-associated alamethicin was investigated by CD spectroscopy as a function of temperature, the data provided evidence for the existence of two forms of the peptide that interconvert as a function of peptide concentration.[15] On the basis of this observation and a large amount of additional experimental data from oriented CD, neutron in-plane scattering, and X-ray diffraction techniques,[16−21] the two-state model has been proposed.[22] At low P/L ratios the peptide associates with the membrane surface and inserts in a transmembrane fashion above a threshold concentration.[16] Correspondingly, a minimal peptide concentration is required for antibiotic and channel activities. Moreover, well-defined water-filled openings were detected by neutron in-plane scattering in bilayers containing transmembrane alamethicin.[17]

However, to our knowledge, direct alamethicin peptide oligomerization has never been detected experimentally, and the exact molecular structure of the pore remains speculative. Therefore, advanced pulsed EPR methods (such as PELDOR or DQC) have been developed and have proven their capacity to access peptide oligomerization.[23] Unfortunately, these approaches, as well as novel solid-state NMR spectroscopy DNP signal enhancement techniques,[24] are only applicable at cryo-temperatures, where the lipid membranes are in the gel or subgel phase, whereas at physiological conditions the membranes are in the fluid phase.

* Corresponding authors. Phone: +7 383 3309150 (S.D.), +33 3 90 24 51 50 (B.B.); fax: +7 383 3307350 (S.D.), +33 3 90 24 51 51 (B.B.); e-mail: dzuba@ns.kinetics.nsc.ru (S.D.), bechinger@chimie.u-strasbg.fr (B.B.).
[†] Russian Academy of Sciences.
[‡] University of Strasbourg.
[§] University of Padova.
[||] University of Manitoba.
[⊥] Leiden University.

10.1021/jp8101805 CCC: $40.75
Published on Web 02/12/2009

Here, we tested the influence of temperature and lipid membrane phase on the alamethicin peptide topology when bound to phospholipid membrane by oriented ^{15}N solid-state NMR spectroscopy and EPR ESEEM techniques. The first technique can be applied at both ambient and reduced temperatures and provides a direct indication of the helix alignment relative to the membrane normal.[25,26] In contrast, the ESEEM technique depends on cryo-temperatures but also provides complementary information on the water exposure of the spin labels.

Solid-state NMR spectroscopy has been used successfully in the past to investigate the 3D-structure, topology, and dynamics of many membrane polypeptides [reviewed in refs 27−30]. In particular, proton-decoupled ^{15}N solid-state NMR spectroscopy has been used to investigate the alignment of helical polypeptides and their orientational distribution. Whereas in oriented samples ^{15}N chemical shifts >180 ppm are indicative of transmembrane alignments of α-helices, values <100 ppm are observed for amphipathic peptides oriented with the helix axis parallel to the membrane surface.[25] Proton-decoupled ^{15}N solid-state NMR spectroscopy of macroscopically oriented samples has been successfully applied to alamethicin bound to POPC or DMPC membranes at P/L molar ratios ranging from 1/8 to 1/237, where the predominant peptide orientation is transmembrane.[31−35]

For the purpose of this study we extended these investigations to gel-state PC membranes and to lipids that have been used during EPR investigations. In this manner we were able to assess the influence of low temperatures and, consequently, a change in lipid membrane phase on the alamethicin peptide orientation when bound to PC membranes. On the one hand, POPC is a major component of eukaryotic membranes, exhibits a gel-to-fluid transition temperature at 271 K, and therefore exists in the fluid phase at room temperature. On the other hand, DPPC is in the gel phase at ambient temperatures, with phase transitions from fluid to ripple at 314.5 K, ripple to gel at 308 K, and gel to subgel at 280 K [reviewed in ref 36]. The phase transition temperatures were slightly shifted and broadened upon addition of alamethicin and salt,[37] but for the present study these effects are of minor importance.

ESEEM is a powerful method to study the access of water molecules to the electron spin labeled sites and, in a fashion complementary to the NMR approach, to determine the immersion depth of spin-labeled peptides. The approach is based on the dependence of anisotropic hyperfine interaction constants of nitroxide spins on the proximity of hydrogens. When deuterated water is used, the influence of water can be clearly distinguished from that of lipid molecules. Furthermore, the deuterons increase the amplitude of ESEEM at the X-band. Since water molecules are less abundant in the hydrophobic core of the membrane, the amplitude of the ESEEM spectrum depends on the depth of the peptide label position relative to the membrane surface. Comparison of these data obtained for peptide analogues spin labeled at different positions provides an indicator of peptide orientation. This method has been successfully employed to study the membrane-bound state of the peptaibol trichogin GA IV.[38] In this work we used the solid-state NMR data to compare the excitation profiles obtained by the ESEEM technique at cryo-temperatures with regard to helix−membrane interactions.

Materials and Methods

Materials. The solution synthesis and characterization of the spin-labeled Glu(OMe)[7,18,19] alamethicin F50/5 analogues Alm1, Alm8, and Alm16 are described in ref 39. The biochemical preparation of ^{15}N uniformly labeled alamethicin (F50/7) has been described previously[40] and results in its uniform labeling with ^{15}N to more than 92%. The peptide sequences are:

Ac-*Aib*-Pro-*Aib*-Ala-*Aib*-*Aib*-Gln-*Aib*-Val-*Aib*-Gly-Leu-*Aib*-Pro-Val-*Aib*-*Aib*-Gln-Gln-Phl (Alm)

Ac-**TOAC^{1}**-Pro-Aib-Ala-*Aib*-Ala-Glu(OMe)-*Aib*-Val-*Aib*-Gly-Leu-*Aib*-Pro-Val-*Aib*-*Aib*-Glu(OMe)-Glu(OMe)-Phl (Alm1)

Ac-*Aib*-Pro-Aib-Ala-*Aib*-Ala-Glu(OMe)-**TOAC^{8}**-Val-*Aib*-Gly-Leu-*Aib*-Pro-Val-*Aib*-*Aib*-Glu(OMe)-Glu(OMe)-Phl (Alm8)

Ac-*Aib*-Pro-Aib-Ala-*Aib*-Ala-Glu(OMe)-*Aib*-Val-*Aib*-Gly-Leu-*Aib*-Pro-Val-**TOAC^{16}**-*Aib*-Glu(OMe)-Glu(OMe)-Phl (Alm16)

The chemical structures of Aib and the TOAC label are shown below:

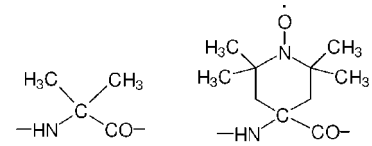

Aib TOAC

As for alamethicin, the more easily synthesized γ-methyl Glu analogs are also functional as channels and aggregate easily.[41−43] The last step in the preparation of the Alm8 and Alm16 analogues involved precipitation from organic solvents. For the Alm1 analogue it was lyophilization. So for Alm1, many more water molecules could remain associated with the peptide, thus resulting in a lower peptide content, and hence, radical content, per sample.

All lipids were from Avanti Polar Lipids, Inc. (Alabaster, AL). For the preparation of buffer solutions, reagent grade chemicals and deuterated water (D_2O) were obtained from Sigma-Aldrich (St. Louis, MO). All commercial products were used without further purification.

Sample Preparation for EPR. To prepare homogeneous mixtures of lipids and peptides, these components were first codissolved in chloroform. The solvent was then evaporated with a stream of nitrogen gas and thereafter by exposure to high vacuum for at least 3 h. The mixture was dispersed in PBS buffer by vortex mixing well-above the phase transition temperature of the membranes (i.e., at 328 K for DPPC and at room temperature for POPC membranes). The hydrated lipid bilayers were briefly sonicated in a bath sonicator (for more homogeneous mixing) and subjected to five rapid freeze−thaw cycles, centrifuged, and concentrated by pelleting in a benchtop centrifuge. After removal of the excess buffer the final water concentration was about 50% w/w. Following this procedure, nonoriented MLVs were obtained.

Sample Preparation for NMR. A homogeneous mixture of lipid and peptide was obtained by codissolving the membrane components in chloroform. To prepare POPC membranes, the solution was spread onto ultra thin cover glasses (9 × 22 mm, Marienfeld, Lauda-Königshofen, Germany), dried first in air or a stream of nitrogen gas and thereafter in high vacuum overnight. For DPPC the protocol was slightly modified to be most closely related to the one used for the preparation of EPR samples. Again, a homogeneous mixture of [U−^{15}N]−Alm and 30 mg of DPPC was first obtained in chloroform, and the solvent was evaporated. Thereafter, 0.2 mL of milliQ water were added, and the resulting suspension was vortexed and sonicated in a bath for 5 min at 55 °C. The resulting milky suspension was loaded onto 25 glass plates, and the water was evaporated in

air and in high vacuum. A small amount (50 μL) of 10 mM Tris buffer (pH 7.5) was equally distributed onto the glass plates. Both the POPC and DPPC membranes were equilibrated at 93% relative humidity. Where necessary, the hydration of the samples was increased by exposure to higher temperatures and 100% relative humidity for 2 h (328 K for DPPC and 310 K for DMPC membranes) before the glass slides were stacked on top of each other.

EPR Spectroscopy. ESEEM experiments were performed on a Bruker ESP 380E pulse X-band EPR spectrometer. A homemade rectangular resonator was used, with a quartz Dewar containing liquid nitrogen. The resonator was overcoupled to obtain a dead time of 100 ns. To improve the signal-to-noise ratio, the three pulse−stimulated echo (π/2-τ-π/2-t_1-π/2-τ-echo) with microwave pulse widths of 16 ns and the microwave power adjusted accordingly was used. The time delay t_1 between the second and the third pulse was incremented while maintaining the separation τ between the first and the second pulse constant at 200 ns to maximize the deuterium modulation. A four-step phase-cycling program was employed to eliminate unwanted echoes.

The time-dependent echo amplitudes, $V(\tau,T)$, were processed to yield standardized ESEEM intensities, according to the previously developed protocol.[44] The average experimental echo decay, $\langle V(\tau,T)\rangle$, was obtained as a smooth function by fitting $\ln(V(\tau,T))$ with a polynomial or a bilinear form. The normalized ESE decay was then obtained as:

$$V_n(\tau, T) = V(\tau, T)/\langle V(\tau, T)\rangle - 1 \quad (1)$$

A complex Fourier transform of this normalized time-domain signal was evaluated numerically as in eq 2,

$$I(\nu_k) = \Delta T \sum_{j=0}^{N} V_n(\tau, T_o + j\Delta T)\exp(-i2\pi\nu_k(T_0 + j\Delta T)) \quad (2)$$

where $\nu_k = k/(N\Delta T)$ with $k = -N/2$ to $+N/2$, and T_0 is a starting time delay between the second and the third pulse in the stimulated echo pulse sequence. The real and imaginary Fourier coefficients were then used to obtain the absolute-value ESEEM spectrum. Although the discrete Fourier transform software supplied with the ELEXSYS FT-EPR spectrometer does not take into account different dwell times, ΔT, in determining amplitudes of the ESEEM spectrum, evaluation according to eq 2 provides spectrometer-independent densities, with the dimensions of time, which can be used for comparing different D_2O-containing systems. The calibration curve representing ESEEM amplitudes for lipids spin-labeled at different positions along the hydrocarbon side chain[44] are presented in Supporting Information Figure S1.

Conventional, continuous-wave EPR spectra were recorded on a Bruker ESP 380E X-band EPR spectrometer with 100 kHz field modulation and 1 G modulation amplitude. A Bruker rectangular resonator was used, with a quartz Dewar containing liquid nitrogen (77 K).

NMR Spectroscopy. Proton-decoupled ^{31}P solid-state NMR spectra were acquired at 161.953 MHz on a Bruker Avance widebore 400 NMR spectrometer equipped with a double resonance flat-coil probe.[45] A phase cycled Hahn-echo pulse sequence[46] with a π/2 pulse of 2.5 μs, a spectral width of 75 kHz, an echo delay of 40 μs, and a recycle delay of 3 s was used. Spectra were referenced externally to 85% H_3PO_4 at 0 ppm.

Proton-decoupled ^{15}N CP spectra of static aligned samples were acquired at 40.54 MHz on a Bruker Avance widebore 400 MHz NMR spectrometer equipped with a double resonance flat-coil probe.[45] An adiabatic CP pulse sequence[47] was used with a spectral width, acquisition time, CP contact time, and recycle delay time of 75 kHz, 3.5 ms, 0.5 ms, and 3 s, respectively. The ^{1}H π/2 pulse and spinal 64 heteronuclear decoupling field strengths were 42 kHz. 40 k scans were accumulated, and the spectra were zero filled to 4096 points. Typically, a 100 Hz exponential line-broadening was applied before Fourier transformation. Spectra were externally referenced to $^{15}NH_4Cl$ at 41.5 ppm. An Oxford temperature control unit was used.

Results

Alamethicin Topology as a Function of Temperature and Membrane Lipid Composition by Solid-state NMR. Figure 1 shows proton-decoupled ^{15}N CP spectra of uniformly ^{15}N labeled alamethicin reconstituted into POPC (E, F) and DPPC (G−J) membranes oriented with the normal of the glass plates parallel to the external magnetic field direction and at peptide concentrations of 1 mol %. The DPPC sample was included in this study as it permits the investigation of the effect of gel phase lipids on alamethicin topology at the same ambient temperature also used for the more physiologically relevant fluid-phase POPC membrane. Solid-state NMR spectra were recorded as a function of temperature. Panels (A) and (D) represent proton-decoupled ^{31}P solid-state NMR spectra of both samples acquired at room temperature.

The proton-decoupled ^{31}P spectrum of POPC (Figure 1A) exhibits one narrow peak at 28 ppm, indicative of highly oriented liquid crystalline lipid bilayers. The proton-decoupled ^{15}N spectrum of [U−^{15}N]−alamethicin exhibits signal intensities predominantly in the 190−230 ppm range (Figure 1E). These chemical shift values correlate with transmembrane orientations of helical peptides.[25]

The spectrum of the same sample recorded at 248 K, that is, below the fluid-to-gel transition temperature of POPC (271 K), is shown in Figure 1F. Although the line is broadened when compared to the room-temperature spectrum (Figure 1E), the chemical shift values indicate that alamethicin remains transmembrane in gel-phase POPC bilayers. The ^{31}P spectrum of oriented POPC lipid bilayers clearly indicates that the lipid membrane is well oriented also at a temperature of 248 K (Figure 1B).

The proton-decoupled ^{31}P spectrum of the gel-phase DPPC membranes at room temperature exhibits a much broader line width and shows spectral intensities ranging from −35 to +40 ppm (Figure 1D). This result strongly suggests that the alignment of the DPPC headgroups is not as homogeneous as in the case of liquid crystalline POPC membranes at the same temperature. The proton-decoupled ^{15}N spectrum of ^{15}N labeled alamethicin when bound to DPPC bilayers (Figure 1H) exhibits all signal intensities in the 60−120 ppm region, indicative of helix alignments perpendicular to the magnetic field direction.[25]

When the temperature is increased to 333 K, the ^{31}P spectrum of this sample reveals well-oriented fluid-phase DPPC bilayers (Figure 1C). At this temperature the maximum of the ^{15}N signal intensity shifts to about 200 ppm (Figure 1G) showing that the peptide predominantly adopts transmembrane orientations in fluid-phase DPPC bilayers. Cooling the same sample to 248 or 223 K, that is, well below the gel-to-subgel phase transition

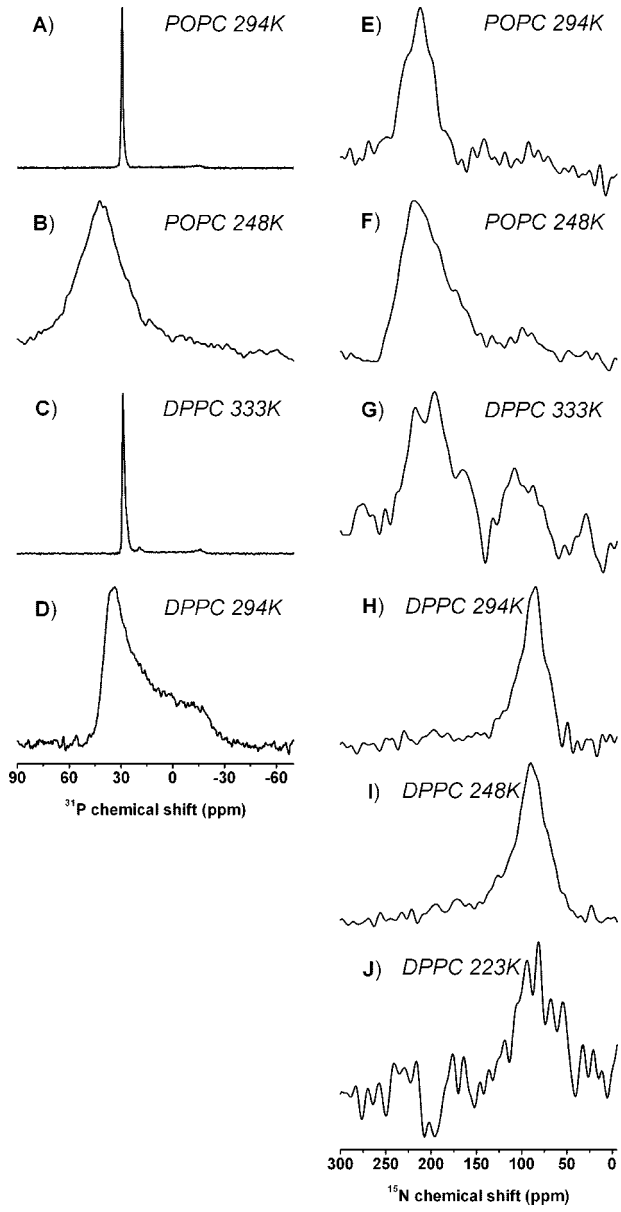

Figure 1. Proton-decoupled solid-state ^{31}P (A−D) and ^{15}N (E−J) NMR spectra of alamethicin labeled uniformly with ^{15}N reconstituted into uniaxially oriented POPC membranes (A, E, F) at a P/L ratio of 1/100 and a temperature of (A, E) 294 K and (F) 248 K; and in DPPC membranes (C, D, G−J) at a P/L ratio of 1/100 and a temperature of (C, G) 333 K, (D, H) 294 K, (I) 248 K, and (J) 223 K. A line-broadening of 300 Hz was applied before Fourier transformation for the spectra on panels B, G, and J. Spectrum B was obtained from pure POPC bilayers at a temperature of 248 K.

temperature for DPPC (280 K), results in the spectra reported in Figures 1I,J. Some broadening is observed when compared to the spectrum obtained at room temperature, and the chemical shift values are indicative of surface orientations of the peptide also under these conditions.

Measurements of the Alamethicin Membrane Penetration by Pulsed EPR at 77 K. ***ESEEM Spectroscopy.*** The ESEEM technique was used to monitor water accessibility and peptide orientation relative to the membrane surface. To enhance the relaxation times of the electron spins, this technique requires recording of the spectra at reduced temperatures, and the ESEEM spectra shown in Figure 2 were therefore recorded at 77 K.

When applied to POPC membranes, the modulus Fourier-transform ESEEM spectra shown in Figure 2A are obtained. The peak intensity is most pronounced for the label at position 1, and labels at positions 8 and 16 are on average buried deeper in the membrane, thereby lowering the signal intensity. A transmembrane alignment was observed for alamethicin in POPC gel-phase by proton-decoupled ^{15}N solid-state NMR spectroscopy (Figure 1E), and the ESEEM data are suggestive that this topology persists also at 77 K.

The ESEEM spectra of TOAC-labeled alamethicin analogues when bound to POPC membranes remain unaffected by the peptide concentration within the range of P/L molar ratios 1/100 (Figure 2A) to 1/20 (not shown). This finding agrees with investigations of POPC-associated alamethicin, labeled uniformly with ^{15}N using proton-decoupled ^{15}N solid-state NMR spectroscopy, where transmembrane alignments were found at P/L ratios of 1/15, 1/100, and 1/237 [Figures 1E, F and refs 31 and 35].

Figure 2B shows the modulus Fourier-transform ESEEM spectra of paramagnetically labeled alamethicin analogues in DPPC membranes at a P/L molar ratio 1:275. Similar data were obtained at P/L molar ratios ranging from 1:275 to 1:50 (not shown). In contrast to POPC membranes, the peak intensity for Alm8 is more pronounced when compared to the Alm1 or Alm16 analogues, indicating that the label at position 8 is closest to the membrane surface, whereas labels at positions 1 and 16 are buried deeper in the bilayer. These results agree well with the in-plane alignment that was observed by solid-state NMR spectroscopy of ^{15}N uniformly labeled alamethicin reconstituted into subgel phase DPPC (Figures 1I,J). It should be noted that the quantitative comparison of the peak intensities observed for different membranes (namely, DPPC and POPC) is not straightforward, but the peptide orientation in POPC membranes is clearly different from the one observed in DPPC.

When the alamethicin concentration in DPPC was increased from 1/50 to 1/20 (Figures 2B and 2C) the labels at positions 8 and 16 become less water accessible, but at the same time the signal of the Alm1 label remains unaffected (Figure 2C). Overall, the ESEEM spectra shown in Figure 2C resemble more closely those of alamethicin reconstituted into POPC membranes (Figure 2A). When an alamethicin/DPPC 1/20 sample deposited onto glass slides is investigated by solid-state NMR spectroscopy at room temperature, both the ^{31}P NMR signal (Figure 3A) of the phospholipids and the ^{15}N spectrum (Figure 3B,C) of the peptide chain are indicative of considerable loss in membrane orientational order (Figure 3).

CW EPR Spectroscopy. CW EPR spectra at 77 K of TOAC-labeled alamethicin analogues bound to lipid membranes at two different concentrations are shown in Figure 4. As at this temperature regime peptide diffusion in the membrane is suppressed, the spectral line width provides an indicator of spin−spin interactions. When alamethicin is reconstituted into DPPC membranes the line widths are similar for all peptide analogues investigated at P/L ratios ranging from 1:275 (Figure 4B) to 1:50 (not shown).

In contrast, the CW EPR spectra at 77 K of TOAC-labeled alamethicin analogues bound to POPC membrane at a 1:100 P/L molar ratio are characterized by line widths that are a function of the label position (Figure 4A). Whereas the lines are broadened for position 8, the label at position 1 exhibits a line width comparable to the one observed after reconstitution into DPPC membranes. The signal arising from position 16 exhibits an intermediate CW EPR line width.

CW EPR spectra at 77 K for TOAC-labeled alamethicin analogues in DPPC at 1/20 P/L molar ratio are shown in Figure 4C. The line-broadening is more pronounced for the label at

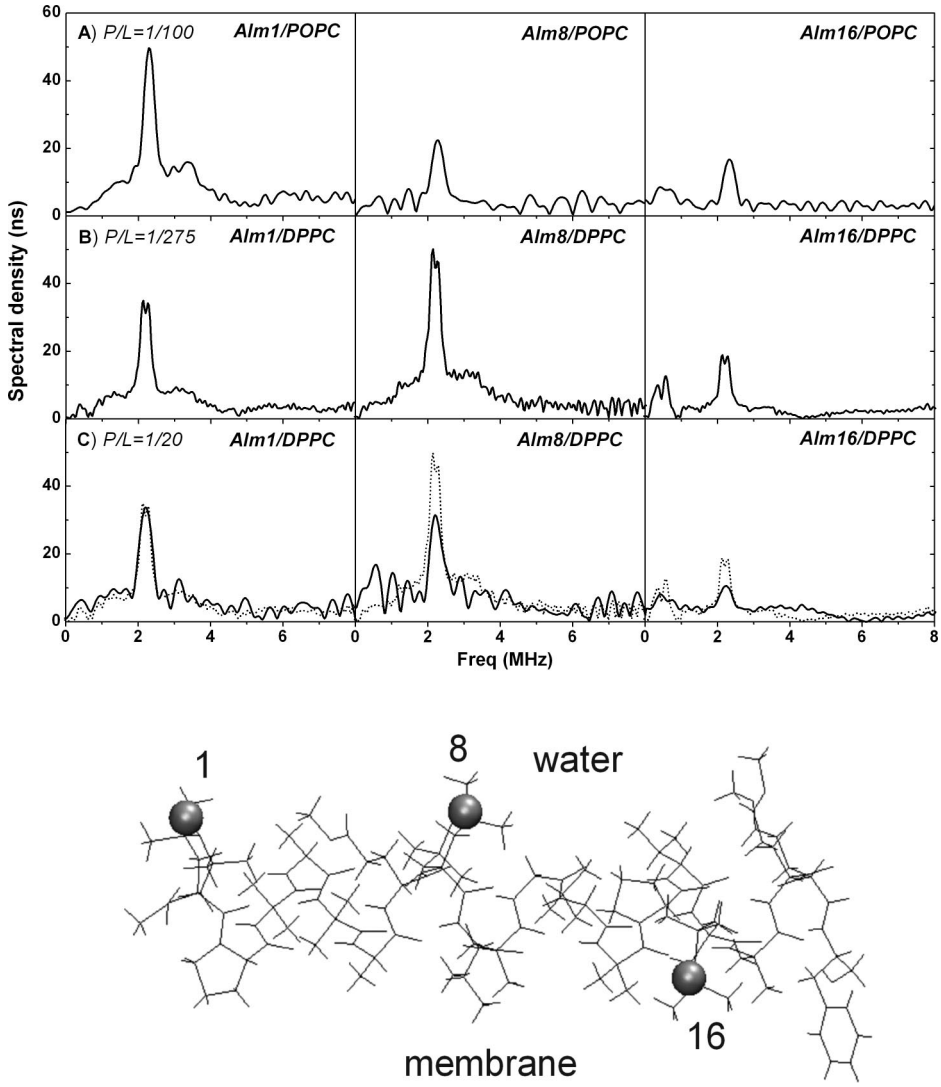

Figure 2. Modulus Fourier-transform ESEEM spectra for TOAC-labeled alamethicin analogues in lipid membrane at different P/L molar ratios. (A) POPC P/L ratio of 1:100, (B) DPPC P/L ratio of 1:275, and (C) DPPC P/L ratio of 1:20. The dotted lines in panel C represent the spectra shown in panel B to facilitate comparison. The location of the nitroxide moieties at positions 1 and 8 are superimposed on the X-ray diffraction structure of alamethicin carrying a TOAC[16] label and Glu(OMe) at positions 7, 18, and 19.[42] Although a positioning of the molecule at the membrane interface as illustrated agrees well with the data shown in panel B, other conformations, arrangements, and/or a conformational heterogeneity are possible.

position 8, even when compared to alamethicin reconstituted into POPC (Figure 4A). To facilitate direct comparison, the CW spectra of alamethicin in POPC at a P/L molar ratio of 1/100 (Figure 4A) are retraced using dotted lines in Figure 4C.

Discussion

Whereas the transmembrane alignment of alamethicin in POPC at room temperature has already been documented,[31,35] its persistence in the gel-phase of the same phospholipid has not been observed previously. Furthermore, the topology of alamethicin and, in particular, its in-plane alignment when interacting with gel-phase DPPC membranes have, to our knowledge, not been reported so far. The ESEEM investigations (Figure 2B) qualitatively confirm the solid-state NMR data (Figure 1H,I) and provide evidence that alamethicin prevails in the surface-oriented state at peptide concentrations of 1 mol % in gel-phase DPPC, well below the liquid crystalline−gel phase transition.

Oriented solid-state NMR spectroscopy has also been used to investigate the transmembrane alignment of alamethicin in DMPC bilayers at P/L molar ratios of 1/8.[32−34] Furthermore, using oriented CD spectroscopy, neutron in-plane scattering, and X-ray diffraction techniques, topological phase diagrams of alamethicin in DPhPC, DOPC, and DPhPE have been established as a function of membrane hydration, temperature, and P/L ratio.[16,17,48,49] Whereas at low alamethicin concentrations the peptides are oriented parallel to the membrane surface, they adopt transmembrane alignments and produce well-defined water-filled pores at high P/L ratios. This finding has been explained by the thinning of the membrane in the presence of in-plane oriented peptides and by the resulting strain on the membrane.[18,20,50] From these observations, the two-state model, that is, an equilibrium between in-plane and transmembrane alamethicin, has been postulated where the transition to the transmembrane topology occurs above a lipid-dependent critical P/L ratio.[22] For DOPC bilayers, which are of comparable thickness as the POPC membranes, the reported threshold occurs at $\leq$0.5 mol % of alamethicin,[16] which is in good agreement with the transmembrane alignments observed at peptide concentrations of 1 mol % (Figure 1E). Related models where

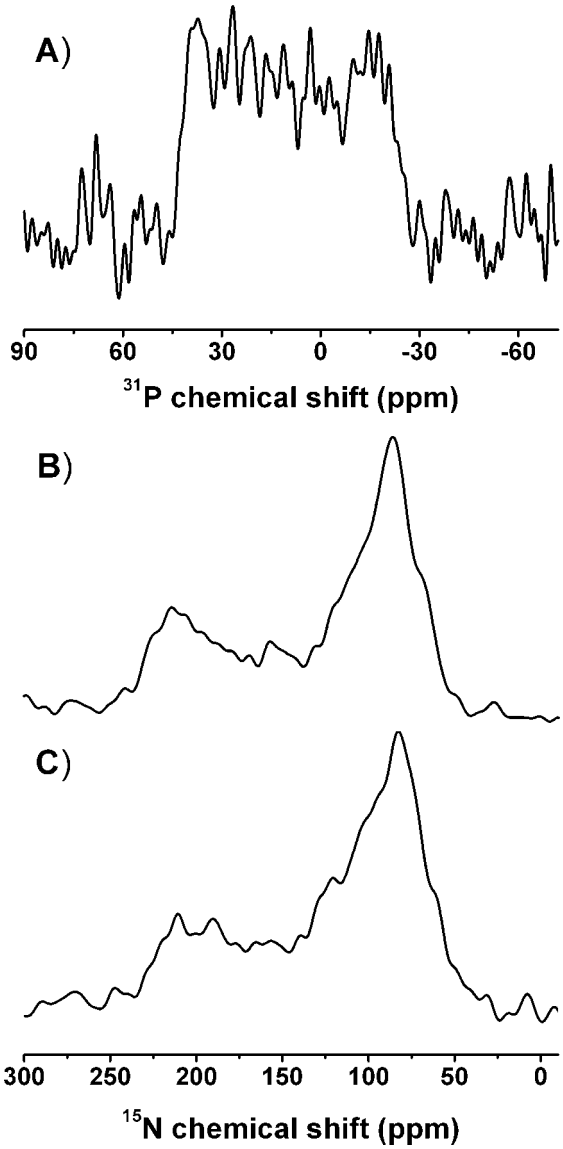

Figure 3. Proton-decoupled solid-state ^{31}P (A) and ^{15}N (B, C) NMR spectra of alamethicin uniformly labeled with ^{15}N and reconstituted into DPPC membranes deposited onto glass plates at a P/L molar ratio of 1/20. The spectra were recorded at room temperature with (A, B) the glass plates oriented with their normal parallel to external magnetic field and (B) perpendicular to the magnetic field direction.

similar types of transitions are responsible for voltage-gating of the channels had been suggested even earlier [reviewed in refs 3 and 51]

Matching the hydrophobic thickness of the membrane and the length of the hydrophobic region of the peptide has been found to be a main requirement for the stable transmembrane insertion of peptaibols.[31] However, other contributions, such as the hydrophobic moment of the peptide or its effects on the lipid fatty acyl chains, are also important.[3,31] The X-ray crystallographic structure of alamethicin exhibits a predominantly α-helical conformation that is 29 Å long.[42,52] The structural data for alamethicin in membrane-like environments are indicative of a relatively stable helix at the N-terminus but a more disordered and flexible C-terminus.[5,53,54] Therefore, this value should only be taken as a rough estimate for the hydrophobic length of the membrane-associated structure. Furthermore, the hydrophobic distance can be shortened, for example, by tilting the helix relative to the membrane normal or by kinks in the structure.[7] On the other hand, it can be elongated by adopting other conformations such as the 3_{10}-helix.[31,35,55]

In the fluid phase, the hydrophobic thickness of DPPC and POPC membranes are 27 Å, a value also observed for DOPC and egg-PC.[56] Interestingly, alamethicin adopts predominantly transmembrane alignments in both systems (Figures 1E−G). When switching to DPPC gel or subgel phases, alamethicin adopts in-plane orientations (Figure 1H−J). This effect is correlated with the reported increase in the hydrophobic thickness of DPPC to 34.4 Å.[56] Whereas in gel-phase DPPC the ^{15}N data indicate that the peptide is well oriented (Figure 1H), the lipid head groups are aligned in a more heterogeneous fashion (Figure 1D) and could, among other possibilities, be explained by structures of toroidal shape.[57] An increase of the hydrophobic thickness in the gel phase seems to be a common feature of bilayers composed of saturated lipid chains.[56] In contrast, the transmembrane orientation of alamethicin persists in gel-phase POPC membranes. The constant *d*-spacing of POPC bilayers when the gel phase (<265.6 K) and the fluid phase (>275 K) are compared to each other[58] suggests that the temperature-dependent changes in membrane hydrophobic thickness are less pronounced for the saturated−monounsaturated POPC bilayers.

A strong dependence of peptide topology on the hydrophobic matching conditions has previously been observed for the 16-residue peptaibol zervamicin II,[31] albeit a detailed comparison with alamethicin suggests additional contributions from the hydrophobic moment of the helices. Furthermore, hydrophobic model sequences adopt stable transmembrane alignments when the peptide is up to 3 Å too short or up to 14 Å too long to match the pure bilayer. These sequences exhibit in-plane alignments when too short and membrane disordering properties when their length much exceeds the hydrophobic thickness of the bilayers.[59] A two-state transition when switching from fluid to gel phase was observed for gramicidin A in DPPC and was explained with hydrophobic mismatch effects.[60]

By comparing the data on the water-exposure of the TOAC labels obtained from ESEEM at 77 K with those from ^{15}N solid-state NMR spectroscopy at low temperatures, it is possible to test if the bulky electron spin labels used in EPR have an effect on the lipid−peptide interactions. Furthermore, by combining both techniques it is feasible to investigate peptide topology over a large range of temperatures (77−333 K).

It should also be noted that the two techniques provide highly complementary information. Whereas the oriented solid-state NMR techniques allow one to measure accurate angular constraints, including tilt and rotational pitch angles in a direct manner,[34,35,61,62] the ESEEM technique provides information on water accessibility of the labeled sites and therefore also on membrane penetration depth. Other EPR techniques have been used to investigate the aggregation state of membrane-associated polypeptides (Figure 3 and refs 38 and 63) and are sensitive to spin−spin interactions within a range of 65 Å.[23] Nuclear spin interactions, like dipolar couplings, can also be used to this end, but they reach over shorter distances, ≤15 Å [reviewed in refs 64, 65]. Although solid-state NMR techniques can be performed at very low temperatures, for example, see ref 66, our NMR probes for oriented biomembrane samples are not designed to this purpose.[45] As the NMR sample size has, for sensitivity reasons, to be considerably increased when compared to EPR, it can be quite demanding to thermally isolate the electronic circuit of the NMR probe from the sample area. In contrast, the spin relaxation of the paramagnetic labels prevents EPR investigations from being performed at biologically relevant

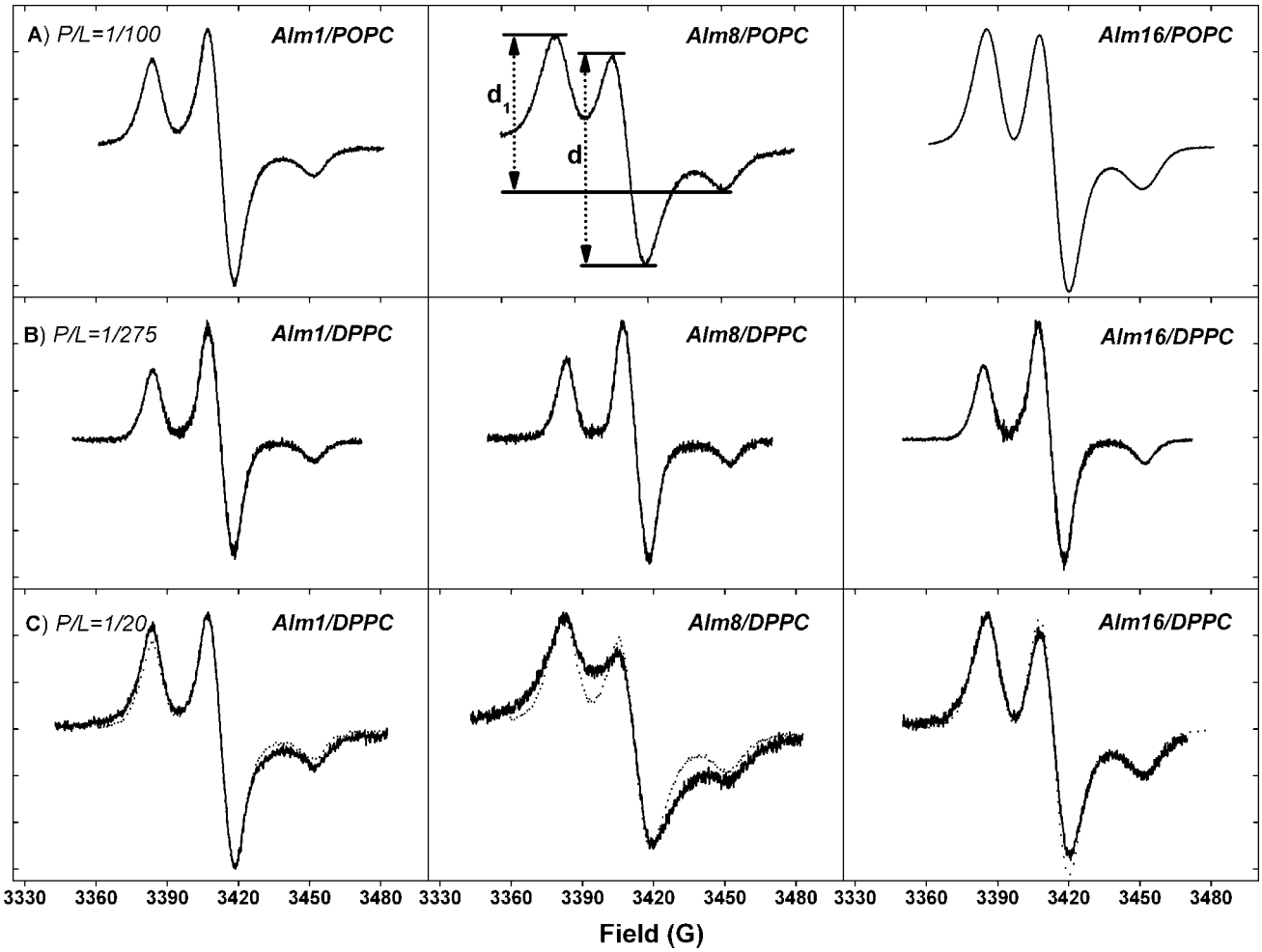

Figure 4. CW EPR spectra of TOAC-labeled alamethicin analogues at 77 K. (A) in POPC at 1:100, (B) in DPPC at 1:275, and (C) in DPPC at 1:20 P/L molar ratios. CW EPR spectra for the corresponding alamethicin analogues bound to POPC membrane at a P/L ratio of 1:275 (panel A) are shown by the dotted line. It should be noted that the peptide concentrations of the Alm1 samples may have been overestimated (cf. Materials and Methods).

(ambient) temperatures. Indeed, we have shown here that alamethicin adopts different topologies in liquid crystalline and gel-state DPPC membranes. However, the POPC bilayer offers itself for the study by either technique as the topological arrangement is, at least qualitatively, unaffected by the bilayer phase transition nor by the TOAC spin labels at the three different positions of the peptide chain. In summary, the two techniques provide highly complementary information covering a large temperature range.

In addition, the direct comparison of oriented solid-state NMR and EPR data has allowed us for the first time to unambiguously identify the ESEEM signature for transmembrane (Figure 2A) and in-plane oriented alamethicin (Figure 2B). Whereas the label at position 1 is always exposed to the water phase, the transmembrane alignment of alamethicin exhibits little water accessibility throughout the central and C-terminal regions of the sequence (Alm8 and Alm16). The signature of the peak intensities in Figure 2A seems to indicate that water accessibility to these central labels is very limited, suggesting a restricted channel volume and/or a mixture of monomers, small nonconducting and larger aggregates, rather than a homogeneous population of large water-filled channels. Within the in-plane oriented helix (Figure 2B), the exposure of individual residues alters with the helical pitch, thereby exposing Alm8 to the water phase but hiding Alm16 in the membrane interior (see the model in Figure 2).

It remains possible that the high peptide concentrations shown in Figure 2C allow such large water-filled cavities or other types of aggregate form. The ESEEM profile observed in this case seems to reflect a degree of water accessibility for Alm8 intermediate to the situations shown in Figures 2A and 2B. In this context it is interesting to note that gel-phase alamethicin/DPPC membranes at P/L ratios of 1/20 exhibit inhomogeneous alignments when investigated by ^{15}N or ^{31}P solid-state NMR spectroscopy (Figure 3), indicating that the peptide disorders the membranes at elevated concentrations. Atomic force microscopy applied to mica-supported gel-phase DPPC membranes in the presence of alamethicin P/L ratios of 1/25 or 1/100 reveals the presence of large openings involving hundreds of peptides with domains of liquid crystalline membranes lining the defects.[37,67] In contrast, well-aligned NMR spectra were obtained previously for alamethicin at elevated concentrations in liquid crystalline DMPC or POPC membranes at ambient temperatures.[31−34]

It should be noted that the water exposure of the label at position 1 seems to contradict an earlier report where CW power saturation EPR was applied to nitroxide-labeled alamethicin in egg-PC.[68] In this study the C-terminus was water-exposed with positions 15 and 9 buried at 1 Å and 11.7 Å from the bilayer surface, respectively. It was calculated that in such an arrangement the N-terminus remains buried deep inside the membrane.[68] The differences in amino acid sequences [analogues of alamethicin-F50/5 vs analogues of F50/7; see ref 4 for nomenclature],

in lipid (20 mM of 50 nm SUVs of egg-PC vs a pellet of MLVs of POPC), in P/L ratio (≤1/500 vs 1/100, addition of peptide after or before vesicle formation), in pH (6.5 vs 7.5), or in temperature (room temperature vs 77 K) can all be responsible for the observed differences. In a related manner, the discrepancies between the topology observed in this work and the one measured in a study using a variety of optical methods[69] probably reflect the characteristics of the peptide derivatives and the variations in experimental conditions. Furthermore, it cannot be excluded that the spin labels themselves affect such a sensitive topological equilibrium and thereby the peptide insertion into the membrane. Finally, the peptide might disrupt the membrane packing and allow access of water from both sides.

Having established the alignment and water exposure of alamethicin, we investigated the membrane-associated peptide by CW EPR at 77 K. In the absence of diffusion, the line width of the EPR signals monitor the dipole−dipole interactions between labeled sites and thus their proximity to one another.[70] The dipolar line-broadening theory that has been developed for the analysis of CW EPR spectra[71] indicates that the line height ratio d_1/d (Figure 4A) can be used to assess the interaction strength. Whereas d_1/d ratios ≤0.4 are characteristic for noninteracting spins, the values observed for Alm8 and Alm16 when bound to POPC membrane at P/L ratios of 1/100 are 0.75 and 0.61, respectively (Figure 4A). Therefore, this result is indicative of dipolar broadening and the existence of aggregated or oligomeric states. The different line broadenings of the labeled positions under identical conditions can be explained, for example, by tilted arrangements of the helices and/or with a kink in the structure.[5,7,53,54] In this manner it is possible that the Alm8 positions would be close to each other, whereas the Alm16 residues are further removed.

In contrast, alamethicin in DPPC at 1 mol % concentrations exhibits d_1/d ratios in the 0.40−0.42 range (Figure 4B) independent of the P/L ratio (in the range 1/275 to 1/50), indicating interspin distances ≥23 Å.[71] It is interesting to note that the broadened CW EPR lines correlate with the experimental conditions where transmembrane topologies are observed for alamethicin. This effect is even more pronounced when the alamethicin sample is reconstituted into DPPC membranes at elevated P/L ratios (Figure 4C), but due to the membrane disordering observed for this sample, interpretation of the spectra remains difficult (Figure 3).

In recent studies the influence of gel- and subgel-phase DPPC, DMPC, and DSPC lipids on the conformation and oligomerization of the membrane-modifying peptide gramicidin A was monitored by CW EPR and DQC EPR methods.[60] A change of the peptide conformation in DPPC and DSPC membranes when switching from the fluid to the gel phase was observed. In contrast, in the case of DMPC, the conformation of membrane-bound gramicidin A remains constant in the range 77−333 K, a temperature range covering several membrane phases. The results were interpreted in terms of match/mismatch between hydrophobic length of the peptide and hydrophobic thickness of bilayers.

Unfortunately, a detailed analysis of the CW EPR spectra in terms of accurate distances and/or aggregation number would depend on a number of assumptions and can, therefore, not be performed reliably. However, self-oligomerization of alamethicin was observed in frozen egg-PC membranes using the PELDOR technique with an oligomer size of 4.[63] The distance distribution for Alm16 was characterized by a broad Gaussian distribution (13 Å wide at half-height) with a maximum at a distance of 23 Å.

In conclusion, our investigations indicate a more stable transmembrane alignment of alamethicin in POPC when compared to DPPC. For the latter bilayer, a switch from a transmembrane alignment to an in-plane disposition has been observed when entering the gel phase. This effect can be explained by the increase in hydrophobic bilayer thickness by about 6 Å and by the resulting hydrophobic mismatch between the bilayer and the peptide. Whereas the DPPC membranes are therefore not suited to obtain biologically relevant data on the interaction of this peptide with membranes using EPR approaches, the topology of alamethicin remains unchanged, at least on a qualitative level, when passing the phase transition temperature of POPC membranes. In addition, the ESEEM technique provides information on the water accessibility and, therefore, membrane penetration depth of the peptides. By comparing the EPR and the NMR techniques, characteristic ESEEM signatures for transmembrane and surface-oriented alamethicin could be identified. The line broadening observed in CW EPR spectra suggests oligomerization of the transmembrane peptide.

Abbreviations Used

Aib	α-aminoisobutyric acid.
CD	circular dichroism.
CP	cross polarization.
CW EPR	continuous wave EPR.
DOPC	1,2-dioleoyl-*sn*-glycero-3-phosphocholine.
DMPC	1,2-myristoyl-*sn*-glycero-3-phosphocholine.
DNP	dynamic nuclear polarization.
DPhPC	1,2-diphytanoyl- *sn*-glycero-3-phosphocholine.
DPhPE	1,2-diphytanoyl- *sn*-glycero-3-phosphoethanolamine.
DPPC	1,2-dipalmitoyl- *sn*-glycero-3-phosphocholine.
DSPC	1,2-stearoyl-*sn*-glycero-3-phosphocholine.
DQC	double quantum coherence.
EPR	electron paramagnetic resonance.
ESEEM	electron spin echo envelope modulation.
MLV	multilamellar vesicles.
NMR	nuclear magnetic resonance.
OMe	methoxy.
PBS	phosphate buffered saline.
PC	phosphatidylcholine.
Phl	phenylalaninol.
PELDOR	pulsed electron−electron double resonance.
P/L	peptide-to-lipid.
POPC	1-palmitoyl-2-oleoyl-*sn*-glycero-3-phosphocholine.
SUV	small unilamellar vesicles.
TOAC	4-amino-1-oxyl-2,2,6,6-tetramethylpiperidine-4-carboxylic acid.

Acknowledgment. The authors thank Dr. A.D. Milov and Dr. P. Bertani for helpful discussions. This work was financially supported by the Dutch-Russian Research Cooperation Program (Netherlands Organization of Scientific Research in collaboration with the Russian Foundation of Basic Research, NWO 047.017.034) and by the Natural Sciences and Engineering Research Council of Canada. E.S.S. greatly thanks the French government fellowship program (BGF) for financial support. The Bechinger group is grateful to the Institute of Supramolecular Chemistry of the University of Strasbourg for hosting the laboratory.

Supporting Information Available: Calibration curve representing ESEEM amplitudes for lipids spin-labeled at different

positions along the hydrocarbon side chain normalized according to eqs 1 and 2 [adapted from ref 44]. This material is available free of charge via the Internet at http://pubs.acs.org.

References and Notes

(1) Woolley, G. A.; Wallace, B. A. *J. Membr. Biol.* **1992**, *129*, 109–136.

(2) Sansom, M. S. *Eur. Biophys. J.* **1993**, *22*, 105–124.

(3) Bechinger, B. *J. Membr. Biol.* **1997**, *156*, 197–211.

(4) Leitgeb, B.; Szekeres, A.; Manczinger, L.; Vagvolgyi, C.; Kredics, L. *Chem. Biodivers.* **2007**, *4*, 1027–1051.

(5) Franklin, J. C.; Ellena, J. F.; Jayasinghe, S.; Kelsh, L. P.; Cafiso, D. S. *Biochemistry* **1994**, *33*, 4036–4045.

(6) Spyracopoulos, L.; Yee, A. A.; O'Neil, J. D. J. *J. Biomol. NMR* **1996**, *7*, 283–294.

(7) North, C. L.; Franklin, J. C.; Bryant, R. G.; Cafiso, D. S. *Biophys. J.* **1994**, *67*, 1861–1866.

(8) Boheim, G.; Kolb, H.-A. *J. Membr. Biol.* **1978**, *38*, 99–150.

(9) Hall, J. E. *Biophys. J.* **1975**, *15*, 934–939.

(10) Stankowski, S.; Schwarz, G. *FEBS Lett.* **1989**, *250*, 556–560.

(11) Archer, S. J.; Ellena, J. F.; Cafiso, D. S. *Biophys. J.* **1991**, *60*, 389–398.

(12) You, S.; Peng, S.; Lien, L.; Breed, J.; Sansom, M. S.; Woolley, G. A. *Biochemistry* **1996**, *35*, 6225–6232.

(13) Barranger-Mathys, M.; Cafiso, D. S. *Biophys. J.* **1994**, *67*, 172–176.

(14) Marsh, D.; Jost, M.; Peggion, C.; Toniolo, C. *Biophys. J.* **2007**, *92*, 473–481.

(15) Woolley, G. A.; Wallace, B. A. *Biochemistry* **1993**, *32*, 9819–9825.

(16) Huang, H. W.; Wu, Y. *Biophys. J.* **1991**, *60*, 1079–1087.

(17) He, K.; Ludtke, S. J.; Heller, W. T.; Huang, H. W. *Biophys. J.* **1996**, *71*, 2669–2679.

(18) Chen, F. Y.; Lee, M. T.; Huang, H. W. *Biophys. J.* **2003**, *84*, 3751–3758.

(19) Spaar, A.; Munster, C.; Salditt, T. *Biophys. J.* **2004**, *87*, 396–407.

(20) Li, C.; Salditt, T. *Biophys. J.* **2006**, *91*, 3285–3300.

(21) Constantin, D.; Brotons, G.; Jarre, A.; Li, C.; Salditt, T. *Biophys. J.* **2007**, *92*, 3978–3987.

(22) Huang, H. W. *Biochim. Biophys. Acta* **2006**, *1758*, 1292–1302.

(23) Tsvetkov, Y. D.; Milov, A. D.; Maryasov, A. G. *Russ. Chem. Rev.* **2008**, *77*, 487–520.

(24) Barnes, A. B.; De Paepe, G.; van der Wel, P. C. A.; Hu, K. N.; Joo, C. G.; Bajaj, V. S.; Mak-Jurkauskas, M. L.; Sirigiri, J. R.; Herzfeld, J.; Temkin, R. J.; Griffin, R. G. *Appl. Magn. Reson.* **2008**, *34*, 237–263.

(25) Bechinger, B.; Sizun, C. *Concept Magn. Res.* **2003**, *18A*, 130–145.

(26) Prongidi-Fix, L.; Bertani, P.; Bechinger, B. *J. Am. Chem. Soc.* **2007**, *129*, 8430–8431.

(27) Bechinger, B.; Kinder, R.; Helmle, M.; Vogt, T. B.; Harzer, U.; Schinzel, S. *Biopolymers* **1999**, *51*, 174–190.

(28) Davis, J. H.; Auger, M. *Prog. NMR Spectrosc.* **1999**, *35*, 1–84.

(29) Watts, A. *Curr. Opin. Biotechnol.* **1999**, *10*, 48–53.

(30) Hong, M. *Acc. Chem. Res.* **2006**, *39*, 176–183.

(31) Bechinger, B.; Skladnev, D. A.; Ogrel, A.; Li, X.; Swischewa, N. V.; Ovchinnikova, T. V.; O'Neil, J. D. J.; Raap, J. *Biochemistry* **2001**, *40*, 9428–9437.

(32) North, C. L.; Barranger-Mathys, M.; Cafiso, D. S. *Biophys. J.* **1995**, *69*, 2392–2397.

(33) Bak, M.; Bywater, R. P.; Hohwy, M.; Thomsen, J. K.; Adelhorst, K.; Jakobsen, H. J.; Sorensen, O. W.; Nielsen, N. C. *Biophys. J.* **2001**, *81*, 1684–1698.

(34) Bertelsen, K.; Pedersen, J. M.; Rasmussen, B. S.; Skrydstrup, T.; Nielsen, N. C.; Vosegaard, T. *J. Am. Chem. Soc.* **2007**, *129*, 14717–14723.

(35) Salnikov, E. S.; Friedrich, H.; Li, X.; Bertani, P.; Reissmann, S.; Hertweck, C.; O'Neil, J. D.; Raap, J.; Bechinger, B. *Biophys. J.* **2009**, *96*, 1–15.

(36) Tristram-Nagle, S.; Nagle, J. F. *Chem. Phys. Lipids* **2004**, *127*, 3–14.

(37) Oliynyk, V.; Kaatze, U.; Heimburg, T. *Biochim. Biophys. Acta* **2007**, *1768*, 236–245.

(38) Salnikov, E. S.; Erilov, D. A.; Milov, A. D.; Tsvetkov, Y. D.; Peggion, C.; Formaggio, F.; Toniolo, C.; Raap, J.; Dzuba, S. A. *Biophys. J.* **2006**, *91*, 1532–1540.

(39) Peggion, C.; Coin, I.; Toniolo, C. *Biopolymers* **2004**, *76*, 485–493.

(40) Yee, A. A.; O'Neil, J. D. *Biochemistry* **1992**, *31*, 3135–3143.

(41) Peggion, C.; Jost, M.; De Borggraeve, W. M.; Crisma, M.; Formaggio, F.; Toniolo, C. *Chem. Biodivers.* **2007**, *4*, 1256–1268.

(42) Crisma, M.; Peggion, C.; Baldini, C.; MacLean, E. J.; Vedovato, N.; Rispoli, G.; Toniolo, C. *Angew. Chem., Int. Ed.* **2007**, *46*, 2047–2050.

(43) Vedovato, N.; Baldini, C.; Toniolo, C.; Rispoli, G. *Chem. Biodivers.* **2007**, *4*, 1338–1346.

(44) Erilov, D. A.; Bartucci, R.; Guzzi, R.; Marsh, D.; Dzuba, S. A.; Sportelli, L. *J. Phys. Chem. B* **2004**, *108*, 4501–4507.

(45) Bechinger, B.; Opella, S. J. *J. Magn. Reson.* **1991**, *95*, 585–588.

(46) Rance, M.; Byrd, R. A. *J. Magn. Reson.* **1983**, *52*, 221–240.

(47) Hediger, S.; Meier, B. H.; Kurur, N. D.; Bodenhausen, G.; Ernst, R. R. *Chem. Phys. Lett.* **1994**, *223*, 283–288.

(48) Vogel, H. *Biochemistry* **1987**, *26*, 4562–4572.

(49) Heller, W. T.; He, K.; Ludtke, S. J.; Harroun, T. A.; Huang, H. W. *Biophys. J.* **1997**, *73*, 239–244.

(50) Lee, M. T.; Chen, F. Y.; Huang, H. W. *Biochemistry* **2004**, *43*, 3590–3599.

(51) Sansom, M. S. P. *Prog. Biophys. Mol. Biol.* **1991**, *55*, 139–235.

(52) Fox, R. O., Jr.; Richards, F. M. *Nature* **1982**, *300*, 325–330.

(53) Yee, A. A.; Babiuk, R.; O'Neil, J. D. J. *Biopolymers* **1995**, *36*, 781–792.

(54) Yee, A. A.; Szymczyna, B.; O'Neil, J. D. *Biochemistry* **1999**, *38*, 6489–6498.

(55) Killian, J. A. *Biochim. Biophys. Acta* **1998**, *1376*, 401–415.

(56) Nagle, J. F.; Tristram-Nagle, S. *Biochim. Biophys. Acta* **2000**, *1469*, 159–195.

(57) Wi, S.; Kim, C. *J. Phys. Chem. B* **2008**, *112*, 11402–11414.

(58) Wang, X.; Quinn, P. J. *Biochim. Biophys. Acta* **2002**, *1567*, 6–12.

(59) Harzer, U.; Bechinger, B. *Biochemistry* **2000**, *39*, 13106–13114.

(60) Dzikovski, B. G.; Borbat, P. P.; Freed, J. H. *Biophys. J.* **2004**, *87*, 3504–3517.

(61) Cross, T. A. *Methods Enzymol.* **1997**, *289*, 672–696.

(62) Aisenbrey, C.; Bechinger, B. *Biochemistry* **2004**, *43*, 10502–10512.

(63) Milov, A. D.; Samoilova, M. I.; Tsvetkov, Y. D.; Jost, M.; Peggion, C.; Formaggio, F.; Crisma, M.; Toniolo, C.; Handgraaf, J. W.; Raap, J. *Chem. Biodivers.* **2007**, *4*, 1275–1298.

(64) Nielsen, N.; Malmendal, A.; Vosegaard, T. *Mol. Membr. Biol.* **2004**, *21*, 129–141.

(65) Hong, M. *Structure* **2006**, *14*, 1731–1740.

(66) Mak-Jurkauskas, M. L.; Bajaj, V. S.; Hornstein, M. K.; Belenky, M.; Griffin, R. G.; Herzfeld, J. *Proc. Natl. Acad. Sci. U S A* **2008**, *105*, 883–888.

(67) Oliynyk, V.; Jager, M.; Heimburg, T.; Buckin, V.; Kaatze, U. *Biophys. Chem.* **2008**, *134*, 168–177.

(68) Barranger-Mathys, M.; Cafiso, D. S. *Biochemistry* **1996**, *35*, 498–505.

(69) Stella, L.; Burattini, M.; Mazzuca, C.; Palleschi, A.; Venanzi, M.; Coin, I.; Peggion, C.; Toniolo, C.; Pispisa, B. *Chem. Biodivers.* **2007**, *4*, 1299–1312.

(70) Steinhoff, H. J.; Radzwill, N.; Thevis, W.; Lenz, V.; Brandenburg, D.; Antson, A.; Dodson, G.; Wollmer, A. *Biophys. J.* **1997**, *73*, 3287–3298.

(71) Farahbakhsh, Z. T.; Huang, Q. L.; Ding, L. L.; Altenbach, C.; Steinhoff, H. J.; Horwitz, J.; Hubbell, W. L. *Biochemistry* **1995**, *34*, 509–516.

JP8101805